Supporting Information

Porphyrin Nanowire Bundles for Efficient Photoconductivity, Photoemission, and Generation of Singlet Oxygens toward Photodynamic Therapy

Tsuneaki Sakurai, Shugo Sakaguchi,† Yuki Takeshita,† Kazuto Kayama, Akifumi Horio, Masaki Sugimoto, Tetsuya Yamaki, Atsuya Chiba, Yuichi Saitoh, Lakshmi B.V.S. Garimella, Devesh Kumar Avasthi, and Shu Seki*

Department of Molecular Engineering, Graduate School of Engineering, Kyoto University, Nishikyo-ku, Kyoto 615-8510, Japan.

Department of Applied Chemistry, Graduate School of Engineering, Osaka University, 2-1 Yamadaoka, Suita, Osaka 565–0871, Japan.

Takasaki Advanced Radiation Research Institute, National Institutes for Quantum and Radiological Science and Technology, 1233 Watanuki-machi, Takasaki, Gunma 370-1292, Japan.

Special Center for Nanoscience, Jawaharlal Nehru University, New Mehrauli Road, New Delhi 110067, India.
Amity Centre for Accelerator based Fundamental and Applied Research, Amity University Uttar Pradesh, Noida 201303, India.

*Correspondence and requests for materials should be addressed to Shu Seki (seki@moleng.kyoto-u.ac.jp).
† These authors contributed equally to this work.

Table of Contents

1. Synthesis

1.1. Summarized Synthetic Schemes

Synthesis of Porphyrin Derivatives 2, 3, 4, 5, and 6.

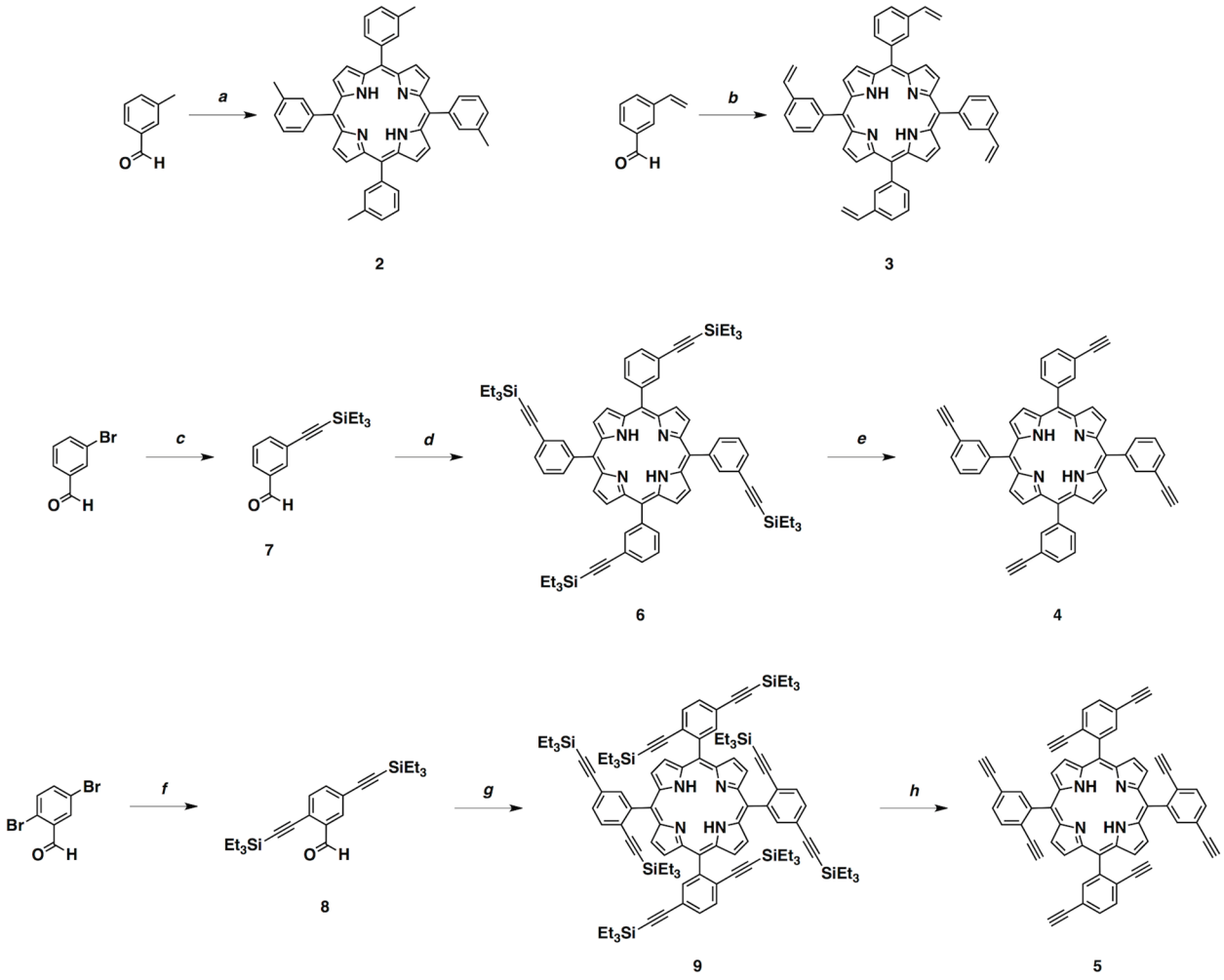

Reagents and Conditions: (a) BF_3•OEt_2, CH_2Cl_2, 25 °C, then DDQ, 25 °C; (b) triethylsilylacetylene, EtN_3, reflux; (c) BF_3•OEt_2, CH_2Cl_2, 25 °C, then DDQ, 25 °C; (d) TBAF, THF, 0 °C; (e) triethylsilylacetylene, EtN_3, reflux; (f) BF_3•OEt_2, CH_2Cl_2, 25 °C, then DDQ, 25 °C; (g) TBAF, THF, 0 °C.

1.2. Synthesis of Compound 2

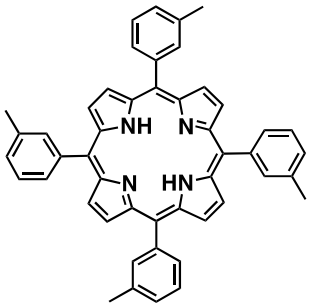

2

To a CH_2Cl_2 solution (700 mL) of a mixture of 3-methylbenzaldehyde (1.24 g, 10.3 mmol) and pyrrole (0.69 g, 10.3 mmol) at 25 °C was added $BF_3 \cdot OEt_2$ (75 μL) and the mixture was stirred for 4 h under N_2. Then, 2,3-dichloro-5,6-dicyano-1,4-benzoquinone (DDQ; 9.35 g, 41.2 mmol) was added and the reaction mixture was stirred for 10 min. The reaction mixture was filtered through alumina gel and evaporated to dryness under reduced pressure. The residue was subjected to column chromatography on silica gel using hexane/$CHCl_3$ (1/1 v/v) as an eluent and evaporated to dryness under reduced pressure. The residue was recrystallized from $CHCl_3$/MeOH, to allow isolation of **2** as reddish purple solid (508 mg, 0.76 mmol, 29%). ^{1}H NMR ($CDCl_3$) δ 8.85 (s, 8H, β-H), 7.99–8.05 (m, 8H, Ar-H), 7.56–7.65 (m, 8H, Ar-H), 2.64 (s, 12H, CH_3), –2.78 (s, 2H, NH); MALDI-TOF MS *m*/*z* calcd. for $C_{48}H_{38}N_4$ $[M]^+$ 670.31, found 670.94.

1.3. Synthesis of Compound 3

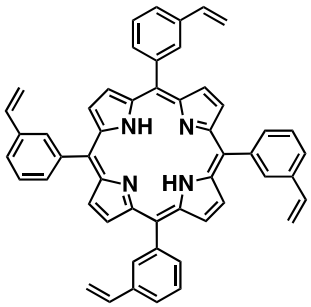

3

To a CH_2Cl_2 solution (1400 mL) of a mixture of 3-vinylbenzaldehyde (2.50 g, 18.9 mmol) and pyrrole (1.27 g, 18.9 mmol) at 25 °C was added $BF_3 \cdot OEt_2$ (150 μL) and the mixture was stirred for 4 h under N_2. Then, DDQ (17.2 g, 75.7 mmol) was added and the reaction mixture was stirred for 10 min. The reaction mixture was filtered through alumina gel and evaporated to

dryness under reduced pressure. The residue was subjected to column chromatography on silica gel using hexane/$CHCl_3$ (1/1 v/v) as an eluent and evaporated to dryness under reduced pressure. The residue was reprecipitated from $CHCl_3$/MeOH, to allow isolation of **3** as reddish purple solid (1.39 g, 1.93 mmol, 41%). ^{1}H NMR ($CDCl_3$) δ 8.87 (s, 8H, β-H), 8.26 (s, 4H, Ar-H), 8.11 (d, J = 7.8 Hz, 4H, Ar-H), 7.84 (d, J = 7.8 Hz, 4H, Ar-H), 7.71 (t, J = 7.6 Hz, 4H, Ar-H), 6.98 (dd, J = 11.0, 17.8 Hz, 4H, C–C*H*=CH_2), 5.96 (d, J = 17.6 Hz, 4H, C–CH=C*H*$_2$), 5.40 (d, J = 10.7 Hz, 4H, C–CH=C*H*$_2$), –2.78 (s, 2H, NH); MALDI-TOF MS m/z calcd. for $C_{52}H_{38}N_4$ $[M]^+$ 718.31, found 718.72.

1.4. Synthesis of Compound 7

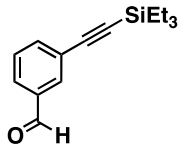

7

To a Et_3N solution (100 mL) of 3-bromobenzaldehyde (3.00 g, 16.2 mmol) were successively added triethylsilylacetylene (3.41 g, 24.3 mmol), $Pd(PPh_3)_4$ (0.94 g, 0.81 mmol), and CuI (0.62 g, 3.24 mmol), and the mixture was refluxed for 3 h under N_2. Then, the reaction mixture was cooled down to 25 °C and poured into hexane (200 mL)/ether (50 mL). The resultant mixture was filtered off from insoluble fractions and evaporated to dryness under reduced pressure. The residue was subjected to column chromatography on silica gel using hexane/CH_2Cl_2 (2/1 v/v) as an eluent, to allow isolation of **7** as pale yellow liquid (3.64 g, 14.9 mmol, 92%). ^{1}H NMR ($CDCl_3$) δ 10.0 (s, 1H, CHO), 7.97 (s, 1H, Ar-H), 7.83 (d, J = 7.8 Hz, 1H, Ar-H), 7.72 (d, J = 7.8 Hz, 1H, Ar-H), 7.48 (t, J = 7.8 Hz, 1H, Ar-H), 0.87–0.89 (t, J = 6.5 Hz, 3H, CH_2).

1.5. Synthesis of Compound 6

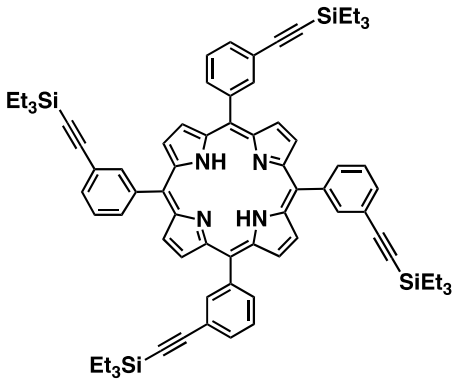

6

To a CH_2Cl_2 solution (1100 mL) of a mixture of **7** (3.76 g, 16.8 mmol) and pyrrole (1.12 g, 16.8 mmol) at 25 °C was added $BF_3 \cdot OEt_2$ (120 μL) and the mixture was stirred for 4 h under N_2. Then, DDQ (9.35 g, 41.2 mmol) was added and the reaction mixture was stirred for 10 min. The reaction mixture was filtered through alumina gel and evaporated to dryness under reduced pressure. The residue was subjected to column chromatography on silica gel using hexane/$CHCl_3$ (1/1 v/v) as an eluent and evaporated to dryness under reduced pressure. The residue was reprecipitated from $CHCl_3$/MeOH, to allow isolation of **6** as reddish purple solid (2.00 g, 1.71 mmol, 41%). ^{1}H NMR ($CDCl_3$) δ 8.84 (s, 8H, β-H), 8.33 (s, 4H, Ar-H), 8.14 (d, J = 7.8 Hz, 4H, Ar-H), 7.90 (d, J = 7.8 Hz, 4H, Ar-H), 7.69 (t, J = 7.6 Hz, 4H, Ar-H), 1.05 (t, J = 7.8 Hz, 36H, CH_3), 0.69 (q, J = 7.8 Hz, 24H, CH_2), –2.86 (s, 2H, NH); MALDI-TOF MS m/z calcd. for $C_{76}H_{86}N_4Si_4$ $[M]^+$ 1166.59, found 1167.457.

1.6. Synthesis of Compound 4

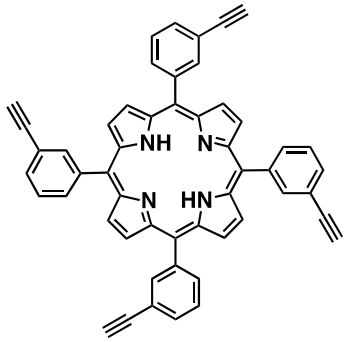

4

To a THF solution (50 mL) of a **6** (0.40 g, 0.34 mmol) at 0 °C was added a THF solution of tetrabutylammonium fluoride (2.0 mL, 1 M), and the mixture was stirred for 12 h under N_2 at

25 °C. Then, the reaction mixture was poured into water and extracted with $CHCl_3$. The organic extract was washed with brine, dried over Na_2SO_4, and evaporated to dryness under reduced pressure. The residue was subjected to column chromatography on silica gel using hexane/$CHCl_3$ (1/1 v/v) as an eluent and evaporated to dryness under reduced pressure. The residue was reprecipitated from $CHCl_3$/MeOH, to allow isolation of **4** as reddish purple solid (0.17 g, 71%). ^{1}H NMR ($CDCl_3$) δ 8.84 (s, 8H, β-H), 8.36 (s, 4H, Ar-H), 8.19 (d, J = 7.8 Hz, 4H, Ar-H), 7.93 (d, J = 7.8 Hz, 4H, Ar-H), 7.72 (t, J = 7.6 Hz, 4H, Ar-H), 3.17 (s, 4H, ≡CH), –2.86 (s, 2H, NH); MALDI-TOF MS m/z calcd. for $C_{52}H_{30}N_4$ $[M]^+$ 710.25, found 710.59.

1.7. Synthesis of Compound 8

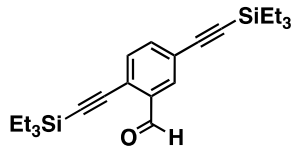

8

To a Et_3N solution (100 mL) of 2,5-dibromobenzaldehyde (2.50 g, 9.47 mmol) were successively added triethylsilylacetylene (2.92 g, 20.8 mmol), $Pd(PPh_3)_4$ (1.1 g, 0.95 mmol), and CuI (0.54 g, 2.84 mmol), and the mixture was refluxed for 12 h under N_2. Then, the reaction mixture was cooled down to 25 °C and poured into hexane (200 mL)/ether (50 mL). The resultant mixture was filtered off from insoluble fractions and evaporated to dryness under reduced pressure. The residue was subjected to column chromatography on silica gel using hexane/$CHCl_3$ (2/1 v/v) as an eluent, to allow isolation of **8** as pale yellow liquid (3.45 g, 9.02 mmol, 95%). ^{1}H NMR ($CDCl_3$) δ 10.5 (s, 1H, CHO), 7.98 (d, J = 2.0 Hz, 1H, Ar-H), 7.59 (dd, J = 2.0, 8.3 Hz, 1H, Ar-H), 7.51 (d, J = 8.3 Hz, 1H, Ar-H), 1.06 (t, J = 7.8 Hz, 9H, CH_3), 1.04 (t, J = 7.8 Hz, 9H, CH_3), 0.71 (q, J = 8.0 Hz, 6H, CH_2), 0.68 (q, J = 8.0 Hz, 6H, CH_2).

1.8. Synthesis of Compound 9

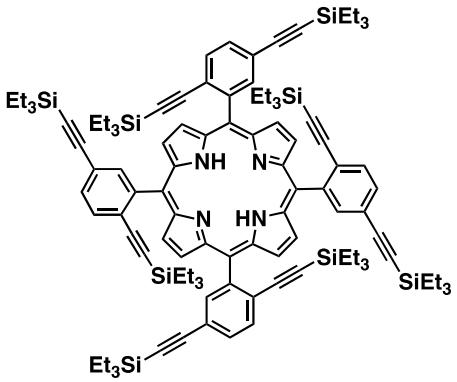

9

To a CH_2Cl_2 solution (700 mL) of a mixture of **8** (3.80 g, 9.93 mmol) and pyrrole (0.67 g, 9.93 mmol) at 25 °C was added $BF_3 \cdot OEt_2$ (75 μL) and the mixture was stirred for 4 h under N_2. Then, DDQ (9.02 g, 39.7 mmol) was added and the reaction mixture was stirred for 10 min. The reaction mixture was filtered through alumina gel and evaporated to dryness under reduced pressure. The residue was subjected to column chromatography on silica gel using hexane/$CHCl_3$ (2/1 v/v) as an eluent and evaporated to dryness under reduced pressure. The residue was reprecipitated from $CHCl_3$/MeOH, to allow isolation of **9** as reddish purple solid (1.02 g, 0.59 mmol, 24%). Compound **9** includes three stereoisomers, affording a complicated NMR spectrum. ^{1}H NMR ($CDCl_3$) δ 8.67–8.73 (s x 3, 8H, β-H), 8.24–8.10 (4H, Ar-H), 7.89–7.78 (8H, Ar-H), 1.05–0.98 (36H, CH_3), 0.71–0.62 (24H, CH_2), –0.17∼–0.82 (60H, CH_2, CH_3), –2.73, –2.77 (s × 2, 2H, NH); MALDI-TOF MS *m*/*z* calcd. for $C_{108}H_{142}N_2Si_8$ $[M]^+$ 1718.94, found 1719.79.

1.9. Synthesis of Compound 5

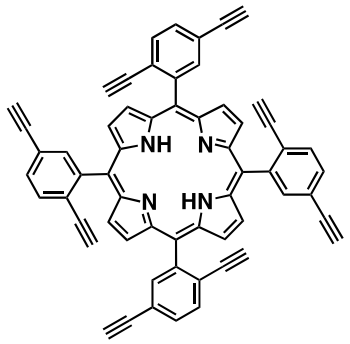

5

To a THF solution (60 mL) of a **3** (0.50 g, 0.29 mmol) at 0 °C was added a THF solution of tetrabutylammonium fluoride (3.5 mL, 1 M), and the mixture was stirred for 6 h under N_2 at 25 °C. Then, the reaction mixture was poured into water and extracted with $CHCl_3$. The organic extract was washed with brine, dried over Na_2SO_4, and evaporated to dryness under reduced pressure. The residue was subjected to column chromatography on silica gel using $CHCl_3$ as an eluent and evaporated to dryness under reduced pressure. The residue was reprecipitated from THF/MeOH, to allow isolation of **5** as reddish brown solid (0.17 g, 73%). Compound **5** includes three stereoisomers, affording a complicated NMR spectrum. ^{1}H NMR (THF-d_8) δ 8.78–8.73 (8H, β-H), 8.36–8.25 (4H, Ar-H), 7.96–7.90 (8H, Ar-H), 3.82–3.80, 2.74–2.65 (8H, ≡CH), –2.70 (s, 2H, NH); MALDI-TOF MS *m*/*z* calcd. for $C_{60}H_{30}N_4$ $[M]^+$ 806.25, found 807.12.

2. Supporting Figures

2.1. Evaluation of Nanowire Radii

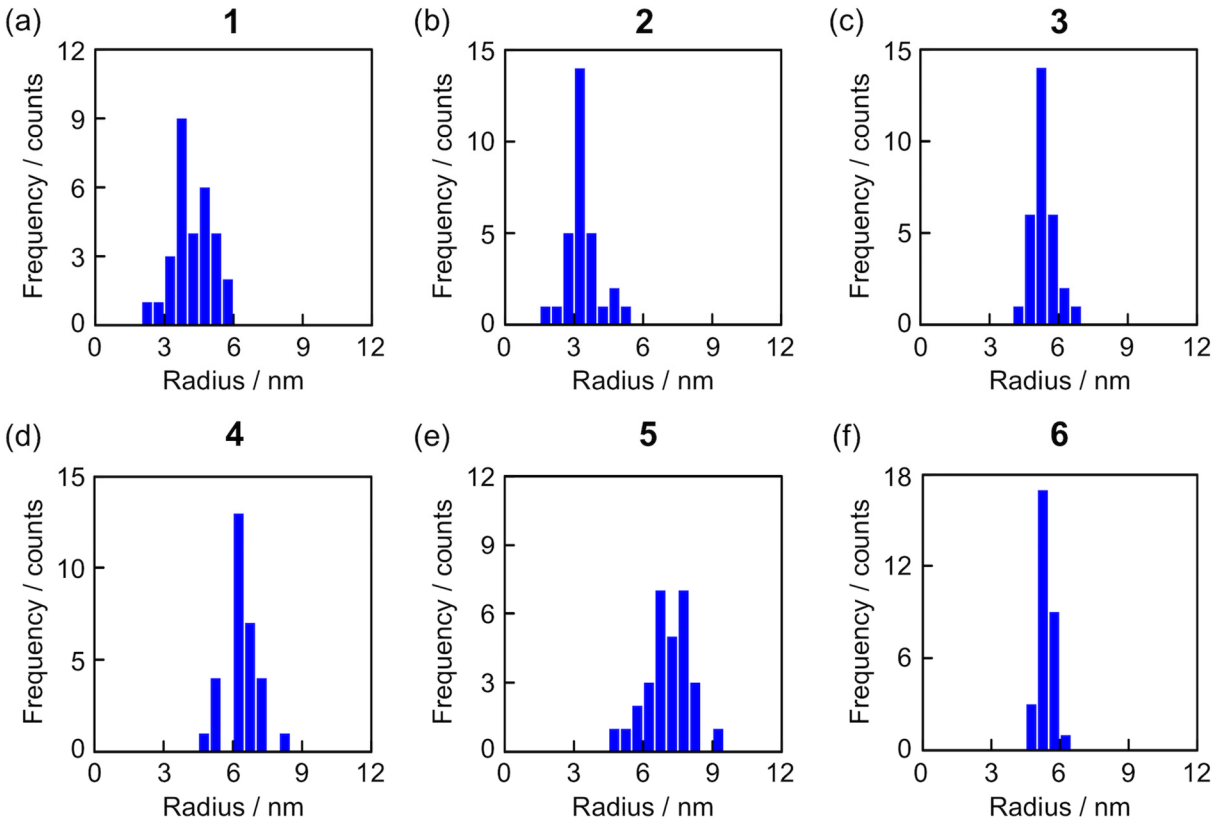

Figure S1. Radius distributions of nanowires fabricated by irradiation with 490 MeV $^{192}Os^{30+}$ particles and development with benzene for **1**–**5** and hexane for **6**.

Table S1. Averaged radii (r) and aspect ratios (r_x/r_y) of nanowires from **1**–**6** fabricated by irradiation with 490 MeV $^{192}Os^{30+}$ particles and development with benzene for **1**–**5** and hexane for **6**.

Starting Compound	r / nm	r_x/r_y
1	4.2 ± 0.9	2.1 ± 0.4
2	3.4 ± 0.7	2.2 ± 0.6
3	5.4 ± 0.5	1.8 ± 0.3
4	6.4 ± 0.7	1.4 ± 0.3
5	7.1 ± 0.9	1.7 ± 0.5
6	5.4 ± 0.4	1.3 ± 0.1

2.2. Evaluation of End-to-End Distances of Nanowires

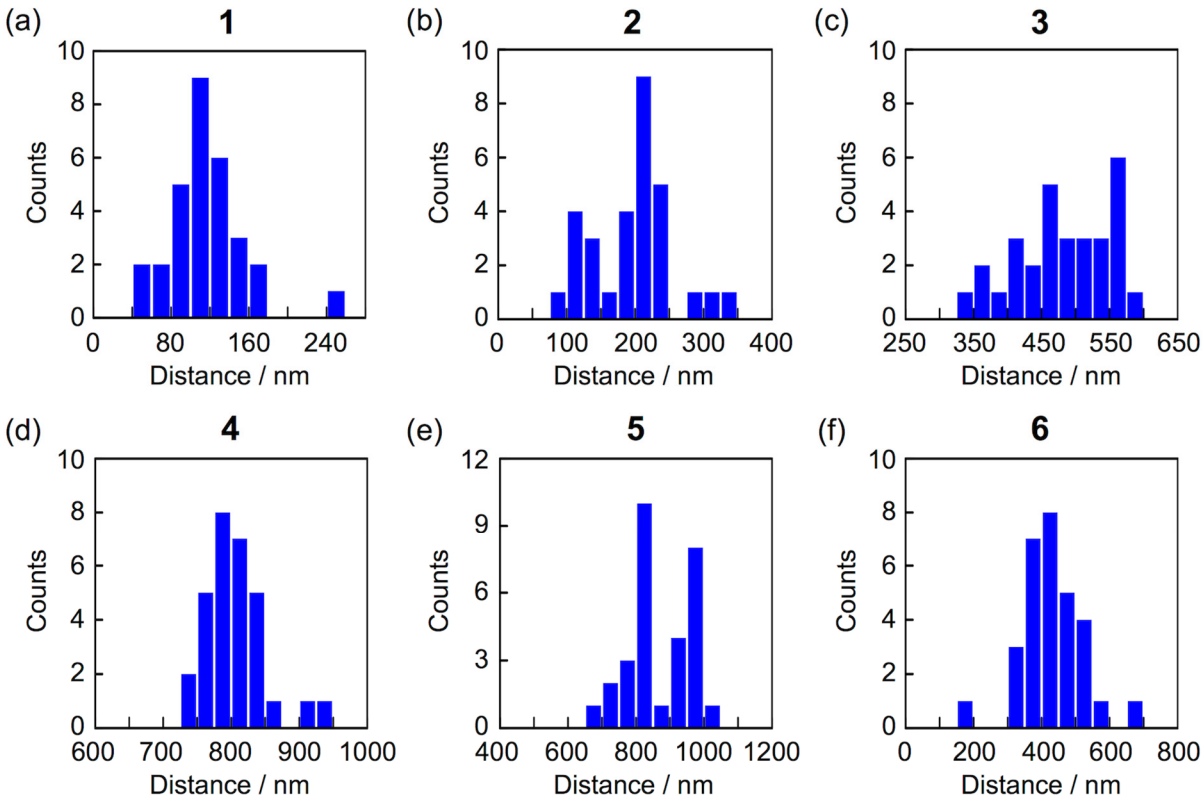

Figure S2. Distributions of end-to-end distances of nanowires fabricated by irradiation with 490 MeV $^{192}Os^{30+}$ particles and development with benzene for **1**–**5** and hexane for **6**. The averaged lengths of nanowires are 163, 294, 628, 831, 926, and 527 for **1**–**6**, respectively (see **Table 1**).

2.3. Evaluation of Rigidity of Nanowires

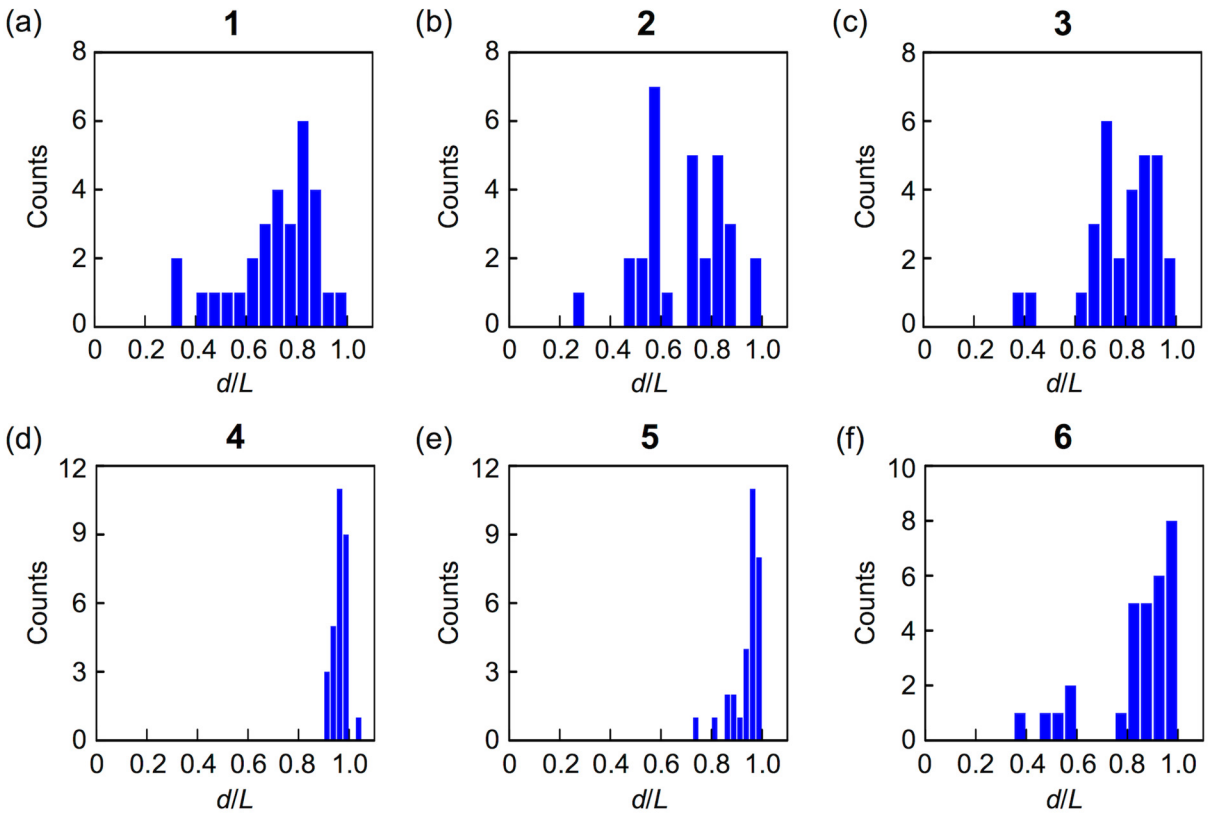

Figure S3. Distributions of d/L values (d: end-to-end distance, L: length) of nanowires for **1**–**6** fabricated by irradiation with 490 MeV $^{192}Os^{30+}$ particles and development with benzene for **1**–**5** and hexane for **6**.

2.4. Scanning Electron Microscopy Images of Nanowires

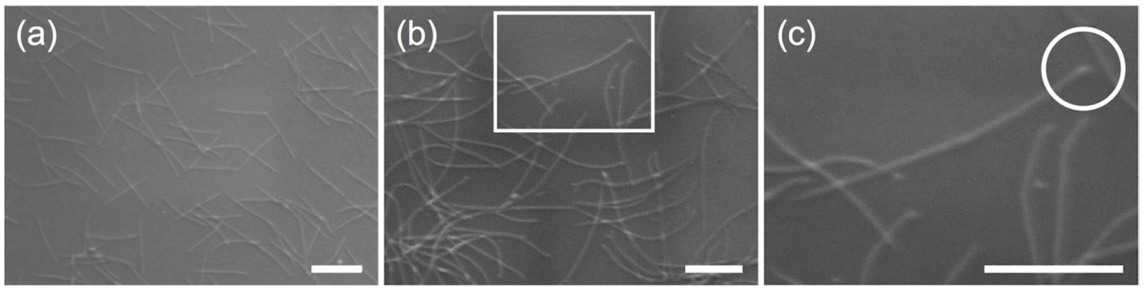

Figure S4. SEM images of nanowires from spincoat film of (a) **4** and dropcast film of (b, c) **5**. The film was irradiated with 490 MeV $^{192}Os^{30+}$ particles at the fluence of 1.0×10^9 ions cm^{-2} and developed with benzene. Scale bars indicate 500 nm. (c) is a magnified image of the square area indicated in (b). Connection of a nanowire terminal with the substrate was visible at the position indicated in the circle in (c).

2.5. Disjointed Nanowires from Substrate by Ultrasonication

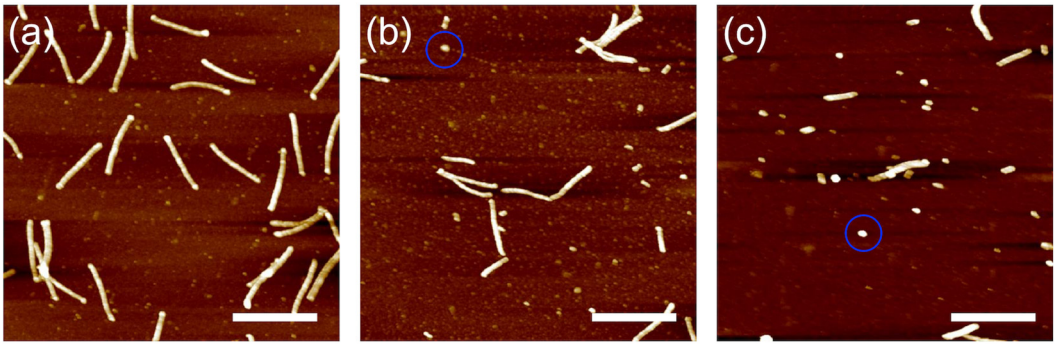

Figure S5. AFM topographic images of nanowires from spincoated film of **4**. The film was irradiated with 490 MeV $^{192}Os^{30+}$ particles at the fluence of 1.0×10^9 ions cm^{-2}, and developed (a) with $CHCl_3$, then with sonication in $CHCl_3$ for (b) 10 min, and (c) further 20 min. Scale bars indicate 500 μm. Blue circles indicate examples of "root"-like nanoobjects. Also fragmented nanowires are seen.

2.6. Nanowire Formation with Lower Energy Ion Irradiation

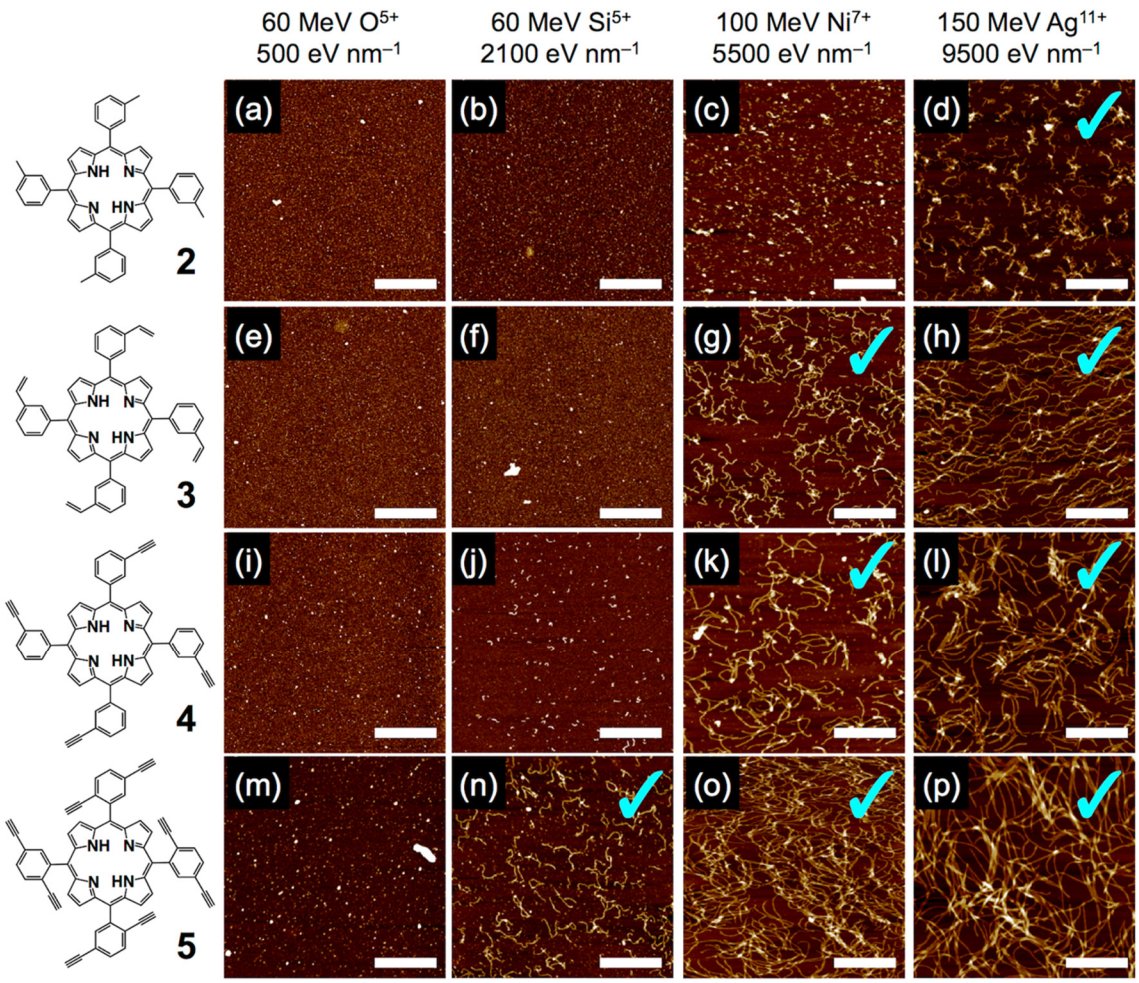

Figure S6. AFM topographic images of nanowires from thin films of (a–d) **2**, (e-h) **3**, (i–l) **4**, and (m–p) **5**. The films were irradiated with (a, e, i, m) 60 MeV $^{16}O^{5+}$, (b, f, j, n) 60 MeV $^{28}Si^{5+}$, (c, g, k, o) 100 MeV $^{58}Ni^{7+}$, and (d, h, l, p) 150 MeV $^{107}Ag^{11+}$ particles at the fluence of 5.0 × 10^9 ions cm^{-2} and developed with *n*-hexane for **2** and benzene for **3**-**5**. Scale bars represent 500 nm. Check marks indicate successful nanowire isolation.

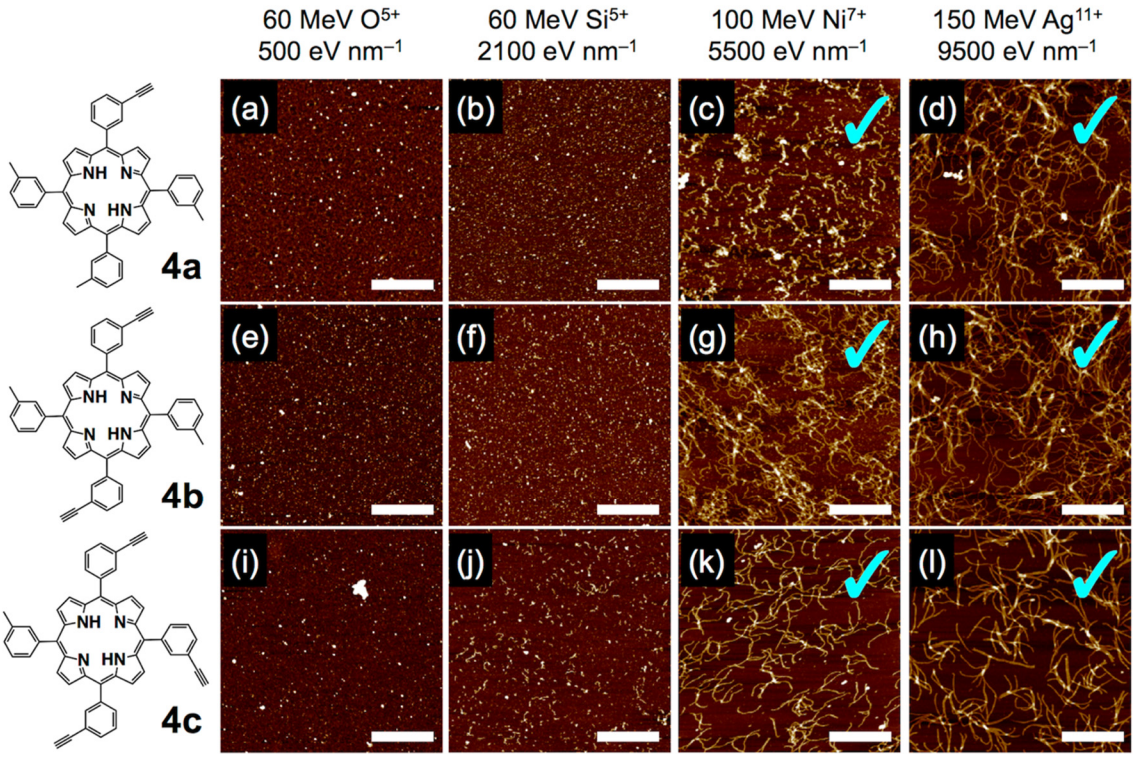

Figure S7. AFM topographic images of nanowires from thin films of reference compounds, (a–d) **4a**, (e–h) **4b**, and (i–l) **4c**. The films were irradiated with (a, e, i,) 60 MeV O^{5+}, (b, f, j) 60 MeV Si^{5+}, (c, g, k) 100 MeV Ni^{7+}, and (d, h, l) 150 MeV Ag^{11+} particles at the fluence of 5.0×10^9 ions cm^{-2} and developed with benzene. Scale bars represent 500 nm. Check marks indicate obvious nanowire isolation.

2.7. Morphology of Nanowires Used for Spectroscopic Measurements

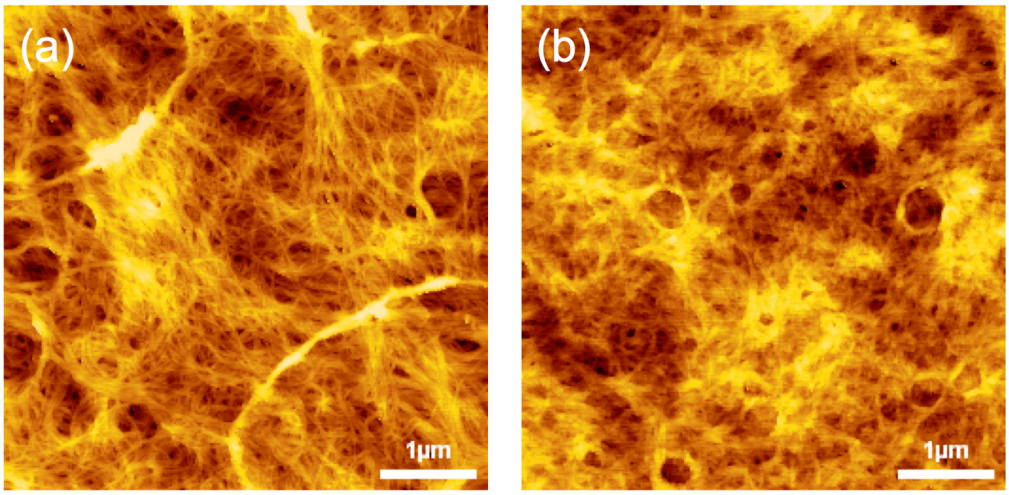

Figure S8. AFM topographic images of nanowires from dropcast films of (a) **4** and (b) **6**. The film was irradiated with 490 MeV $^{192}Os^{30+}$ particles at the fluence of 1.0×10^{10} ions cm^{-2}, and developed with $CHCl_3$ for (a) and *n*-hexane for (b). Scale bars indicate 1 μm.

2.8. Absorption, Excitation, and Emission Spectra of Porphyrin Nanowires

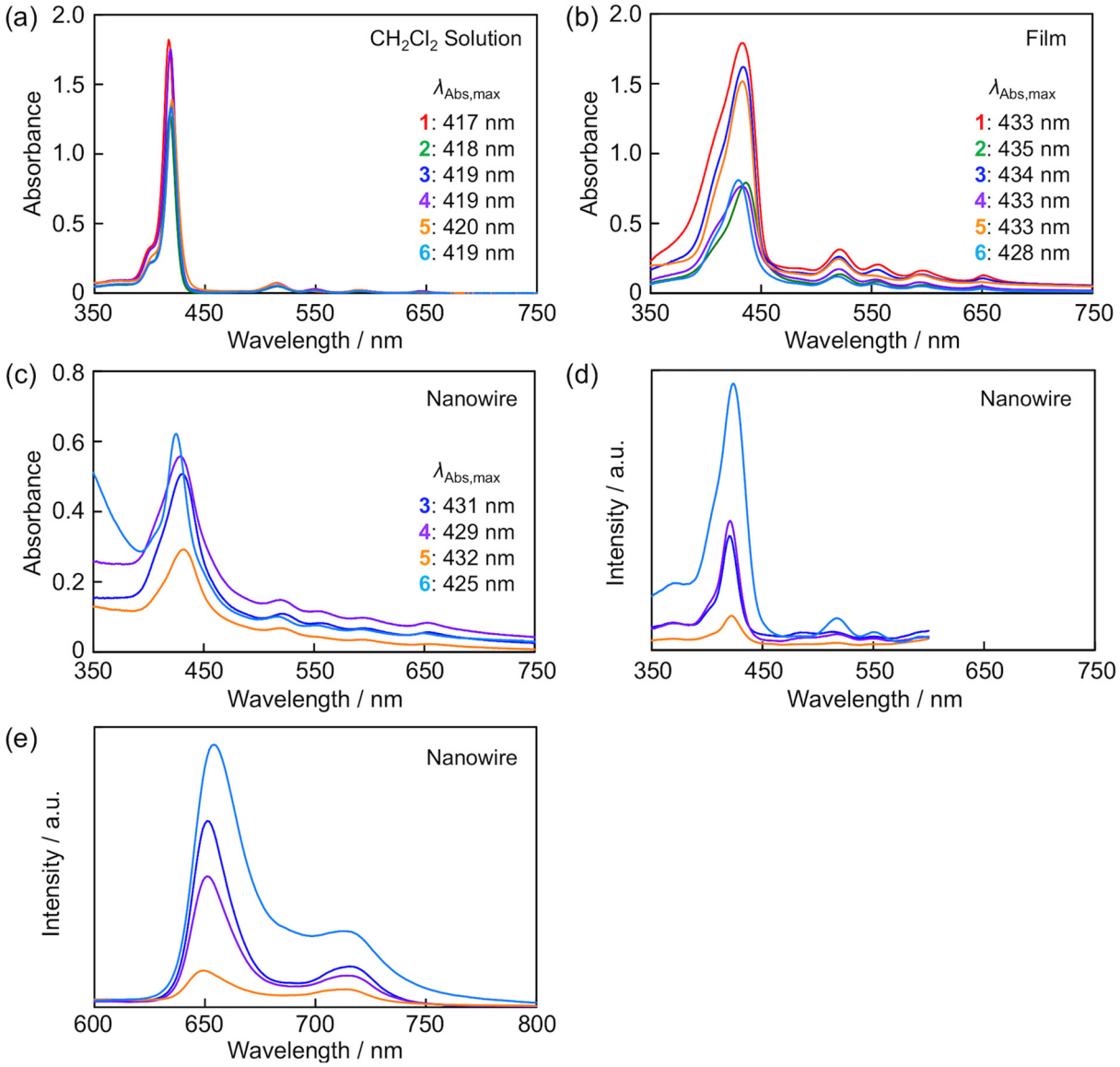

Figure S9. Electronic absorption spectra with wavelength of absorption maxima of (a) CH_2Cl_2 solution, (b) spin-coated thin film, and (c) bundled nanowires for **1** (red), **2** (green), **3** (blue), **4** (purple), **5** (orange), and **6** (pale blue). (d) Excitation (λ_{em} = 651 nm) and (e) emission (λ_{ex} = 420 nm) spectra of bundled nanowires from **3** (blue), **4** (purple), **5** (orange), and **6** (pale blue). The relatively low solubility of **1** and **2** caused a trouble to obtain only thin films and thus yielded nanowires with short lengths, which results in the low spectroscopic sensitivity insufficient for characterizations. Different baselines in (c) are due to the scattering of the incident light.

2.9. Morphology of Nanowires by Stepwise Developments

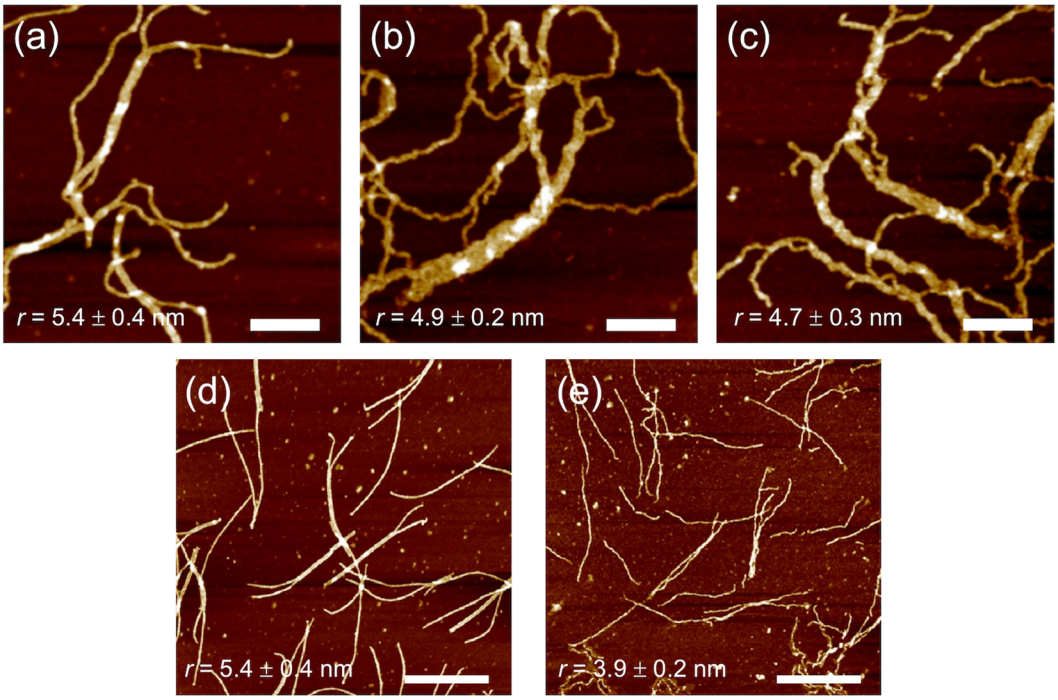

Figure S10. AFM topographic images and corresponding average cross-sectional radius of nanowires from spincoated film of **6**. The film was irradiated with 490 MeV $^{192}Os^{30+}$ particles at the fluence of 1.0×10^9 ions cm^{-2}, and developed initially (a) with *n*-hexane, then with $CHCl_3$ for (b) 30 s, and (c) further 20 min. A different rot sample was confirmed with the development condition with (d) *n*-hexane and (e) then $CHCl_3$ for 30 min. Scale bars indicate 200 and 500 nm for (a–c) and (d,e), respectively.

2.10. Absorption Spectral Changes by Stepwise Developments

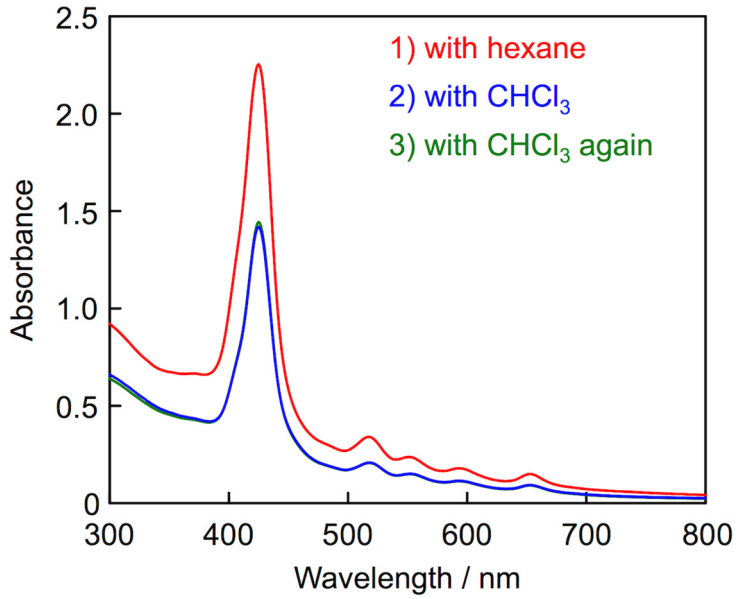

Figure S11. Electronic absorption spectra of nanowires from **6** on quartz plate. Spectra were recorded after development with hexane (red), and then with $CHCl_3$ for 10 min (blue), followed by an additional dipping in $CHCl_3$ for 1 h (green). Nanowires were fabricated by irradiation with 490 MeV $^{192}Os^{30+}$ particles at the fluence of 1.0×10^{10} ions cm^{-2}.

2.11. Size Exclusion Chromatography of Soluble Parts of Porphyrin Nanowires

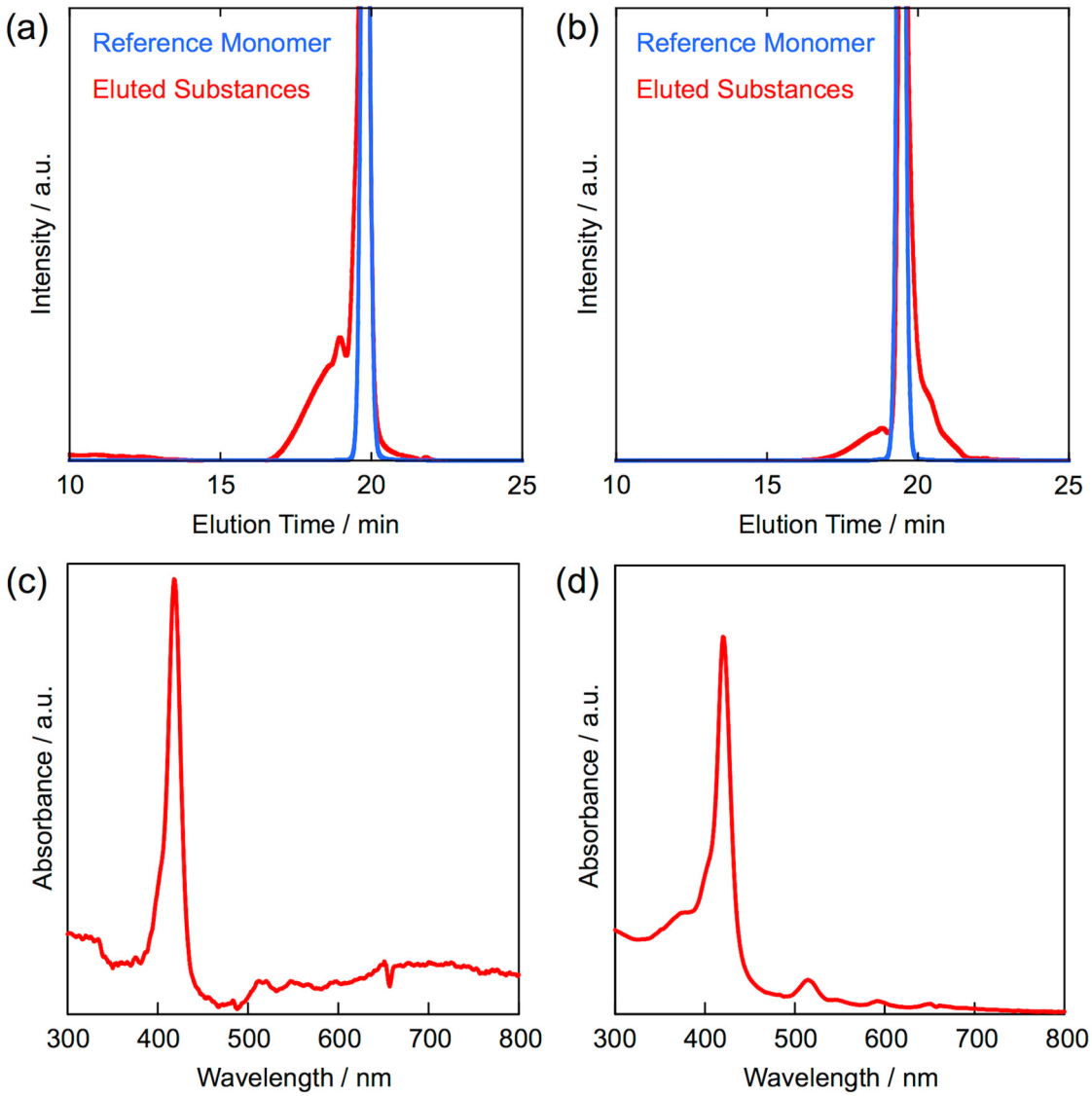

Figure S12. Analytical SEC profiles of monomers (blue) and soluble fractions of their nanowires (red) in THF for (a) **4** and (b) **5**. The formation of nanowires was confirmed by AFM after irradiation with 490 MeV $^{192}Os^{30+}$ at a fluence of 1×10^{10} ions cm^{-2} and subsequent development of the dropcast films of each compound with benzene. Then the nanowires on the Si substrate was immersed in THF, sonicated, filtered from insoluble fraction and then injected into an analytical SEC system using THF as an eluent. Retention time was monitored by UV light at 420 nm. UV-vis absorption spectra of eluted fraction corresponding to the retention peaks in the SEC trace at (c) 19.0 min for the eluted substances in (a) and (d) 18.4 min for the eluted substances in (b).

2.12. AFM Images of Nanowires from Other Ethynyl-Modified Compounds

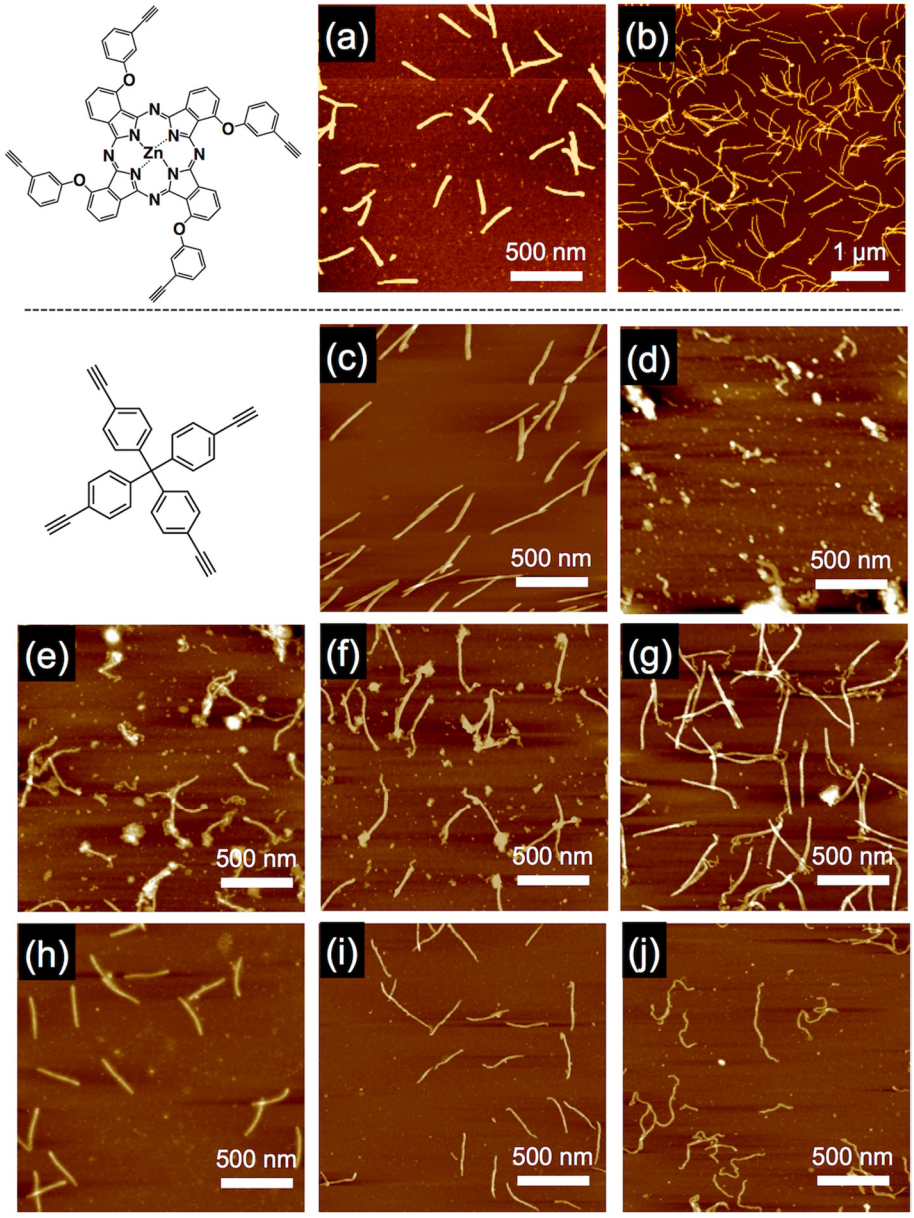

Figure S13. AFM topographic images of nanowires from ethynyl-modified (a,b) phthalocyanine and (c–g) tetraphenylmethane -based compounds. The spin-coated films were irradiated with (a–c) 490 MeV $^{192}Os^{30+}$, (d) 1.5 MeV Al_1, (e) 3.0 MeV Al_2, (f) 4.5 MeV Al_3, (g) 6.0 MeV Al_4, (h) 150 MeV $^{107}Ag^{11+}$, (i) 100 MeV $^{58}Ni^{7+}$, and (j) 60 MeV $^{28}Si^{5+}$, at a fluence of 1×10^9 and 2×10^9 ions cm^{-2} for (a, c–j) and (b), respectively, and then developed with (a,b) benzene or (c–j) toluene.

2.13. Flash-Photolysis Time-Resolved Microwave Conductivity Measurements

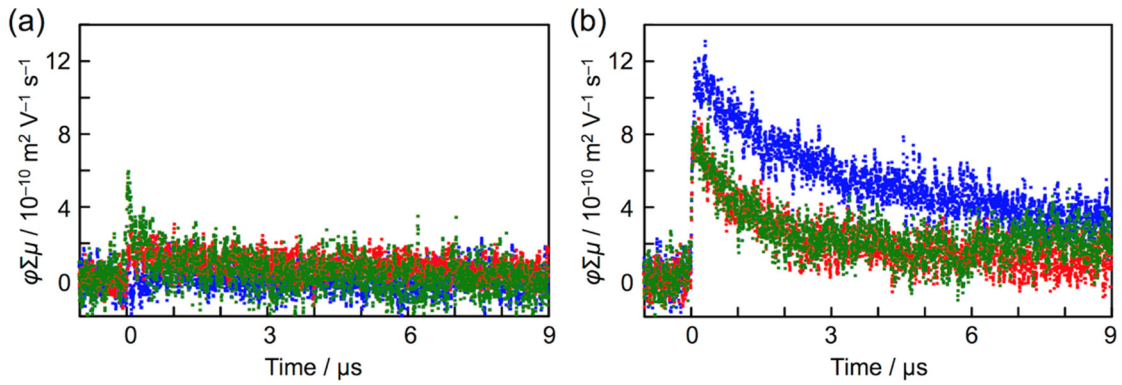

Figure S14. Conductivity transients of **3** (red), **4** (green), and **6** (blue) in (a) thin films and (b) nanowires. Nanowires were fabricated by irradiation with 490 MeV $^{192}Os^{30+}$ particles at the fluence of 1.0×10^{10} ions cm^{-2} and development with benzene.

2.14. AFM Image of Silver Nanoparticle

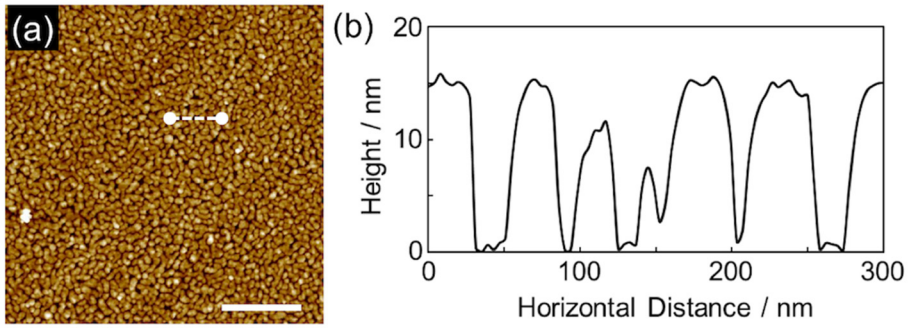

Figure S15. (a) AFM topographic image and (b) height profile (indicated as white dashed line in (a)) of Ag nanoparticles grown on quartz substrates. Scale bar in (a) represents 500 nm.